Reduction of the unnecessary dose from the over-range area with a spiral dynamic *z*-collimator: comparison of beam pitch and detector coverage with 128-detector row CT

Takashi Shirasaka · Yoshinori Funama · Mutsukazu Hayashi ·
Shinichi Awamoto · Masatoshi Kondo · Yasuhiko Nakamura ·
Masamitsu Hatakenaka · Hiroshi Honda

Abstract Our purpose in this study was to assess the radiation dose reduction and the actual exposed scan length of over-range areas using a spiral dynamic *z*-collimator at different beam pitches and detector coverage. Using glass rod dosimeters, we measured the unilateral over-range scan dose between the beginning of the planned scan range and the beginning of the actual exposed scan range. Scanning was performed at detector coverage of 80.0 and 40.0 mm, with and without the spiral dynamic *z*-collimator. The dose-saving ratio was calculated as the ratio of the unnecessary over-range dose, with and without the spiral dynamic *z*-collimator. In 80.0 mm detector coverage without the spiral dynamic *z*-collimator, the actual exposed scan length for the over-range area was 108, 120, and 126 mm, corresponding to a beam pitch of 0.60, 0.80, and 0.99, respectively. With the spiral dynamic *z*-collimator, the actual exposed scan length for the over-range area was 48, 66, and 84 mm with a beam pitch of 0.60, 0.80, and 0.99, respectively. The dose-saving ratios with and without the spiral dynamic *z*-collimator for a beam pitch of 0.60,

0.80, and 0.99 were 35.07, 24.76, and 13.51%, respectively. With 40.0 mm detector coverage, the dose-saving ratios with and without the spiral dynamic *z*-collimator had the highest value of 27.23% with a low beam pitch of 0.60. The spiral dynamic *z*-collimator is important for a reduction in the unnecessary over-range dose and makes it possible to reduce the unnecessary dose by means of a lower beam pitch.

1 Introduction

CT scanners using wide range coverage, such as a 128-detector row with 80.0 mm detector coverage or a 320-detector row with 160.0 mm detector coverage, have recently become available. These scanners provide rapid and wide coverage scanning compared with the current most widely used CT scanners. However, the potential for an unnecessary dose from the over-range area is a critical issue with increasing detector coverage [1–6]. Because, in the helical scan mode, the reconstruction algorithm requires additional raw data on both sides of the planned scan range, extra rotations outside the intended scan range are needed for adequate image reconstruction [7, 8]. In addition, any unnecessary dose due to the extraneous area of coverage does not contribute to imaging, but only increases the patient radiation dose. van der Molen and Geleijns [5] reported that over-ranging may lead to substantial, but unnoticed exposure of radiosensitive organs.

To reduce the unnecessary dose from the over-range area, a spiral dynamic *z*-collimator has been implemented

T. Shirasaka (✉) · M. Hayashi · S. Awamoto · M. Kondo ·
Y. Nakamura
Department of Radiological Technology,
Kyushu University Hospital, 3-1-1 Maidashi,
Higashi-ku, Fukuoka, Fukuoka 812-8582, Japan
e-mail: shirasa@med.kyushu-u.ac.jp

Y. Funama
Department of Medical Physics, Faculty of Life Sciences,
Kumamoto University, 4-24-1 Kuhonji,
Kumamoto 862-0976, Japan

M. Hatakenaka · H. Honda
Department of Clinical Radiology, Graduate School
of Medical Sciences, Kyushu University, 3-1-1 Maidashi,
Higashi-ku, Fukuoka, Fukuoka 812-8582, Japan

on CT scanners [9, 10]. The spiral dynamic z-collimator can asymmetrically shape the X-ray profile geometry in the z-direction and achieve a reduction in the radiation dose for the over-range area. In particular, the spiral dynamic z-collimator is useful for achieving wide coverage with the CT scanner on helical scanning. Walker et al. [10] reported the usefulness of the spiral dynamic z-collimator; the mean relative effective dose reduction was 11.7 and 24.3% with and without the spiral dynamic z-collimator, corresponding to detector coverage of 40.0 and 80.0 mm, respectively, in cardiac CT angiography. When the spiral dynamic z-collimator is used, the dose-saving ratio for the over-range area has an influence on the beam pitch and detector coverage.

In this study, we focused on the difference in the dose-saving ratio with variations in beam pitch and detector coverage in the clinical situation. In particular, this will be applicable to abdominal CT scans. This is because radiosensitive organs, such as the female breast and human gonads, are present at the boundary of the abdominal CT scan and are typically exposed any over-range area dose on helical scanning. In addition, abdominal dynamic CT scans with contrast media are required in multiphase scanning and contribute to increase in the over-range dose.

Our purpose in this study was to assess the radiation dose reduction and the actual exposed scan length of the over-range areas using the spiral dynamic z-collimator at different beam pitches and detector coverage.

2 Materials and methods

2.1 Definition of over-range

We defined the difference between the planned and actual exposed scan range as the over-range, although two definitions of over-range are in common use as follows: the difference between the actual exposed scan range and the planned scan range and the difference between the actual exposed scan range and the imaged scan range [5]. Figure 1 shows the simplified depiction of the over-range components and the definitions in helical CT scanning. To the planned scan range, one section width is automatically added, so that the imaged scan range is slightly longer. Extra rotations needed for image reconstruction are added to the planned scan range, resulting in a longer exposed scan range. For calculation of the unilateral over-range scan dose, the distance between the beginning of the imaged scan range and the beginning of the actual exposed scan range (actual exposed scan length for the over-range area) was calculated as the unilateral over-range scan dose (Fig. 1).

2.2 CT scanning

A 128-detector row CT scanner (Brilliance iCT, Philips Healthcare, Cleveland, OH, USA) was used in the present study. Scanning was performed at two detector coverage ranges, at 80.0 mm with a 128-detector row and at 40.0 mm with a 64-detector row, with and without the spiral dynamic z-collimator (Eclipse DoseRight Collimator, Brilliance iCT, Philips Healthcare, Cleveland, OH, USA). The scanning parameters were as follows: detector configuration, 0.625 mm (detector collimation); image thickness, 5.0 mm; section interval, 5.0 mm; display field of view, 32.0 cm; tube voltage, 120 kV; rotation time, 0.5 s; volume CT dose index (CTDIvol), 12.4 mGy; and scan length, 200 mm. Effective current–time products, 200 and 184 effective mAs, were used for the 80.0 and 40.0 mm detectors, respectively. When we input the effective current–time product, the actual tube current is automatically adjusted to take account of changes in pitch, making the dose within the imaged volume effectively independent of pitch [11]. Three beam pitches (table speed per rotation/beam width) were used: at 0.60, 0.80 and 0.99, for the 80.0- and 40.0-mm coverage ranges, respectively, in consideration of the clinical situation.

2.3 Actual scan doses with radiophotoluminescent glass rod dosimeters at over-range area

The actual scan doses that were delivered to over-range areas were measured with radiophotoluminescent glass rod dosimeters (GRDs: GD-301, Asahi Techno Glass Corporation, Shizuoka, Japan) from the beginning of the actual exposed scan range to the beginning of the planned scan range [1, 12]. We measured an absorbed dose to air using GRDs by comparison with a reference ionization chamber (0.2 cm^3, PTW, Freiburg, Germany) at 58.3 keV in advance, and we determined the calibration factor. Thirty-one GRDs were set up consecutively at 6.0 mm distance apart and at the center position of the scanning area along the z-direction. The long axis of the GRDs was parallel to the z-direction. The GRDs were lined up on the foamed polyethylene board to reduce some of the scattered radiation from the patient couch of the CT scanner.

We scanned 10 times repeatedly with the same GRDs in the same scan length and measured the radiation dose. We also performed the same scanning at three different times, and we calculated the mean value obtained at the three measurements. In total, 1116 GRDs (31 GRDs × 3 times × 3 beam pitch × 2 detector coverage ranges × with and without a spiral dynamic z-collimator) were used in this study. The dose values obtained with the GRDs were automatically read out on the FGD-1000 reader (Asahi Techno Glass Corporation, Shizuoka, Japan). From the mean value, the

Fig. 1 Definition of over-range: the difference between the planned and actual exposed scan range
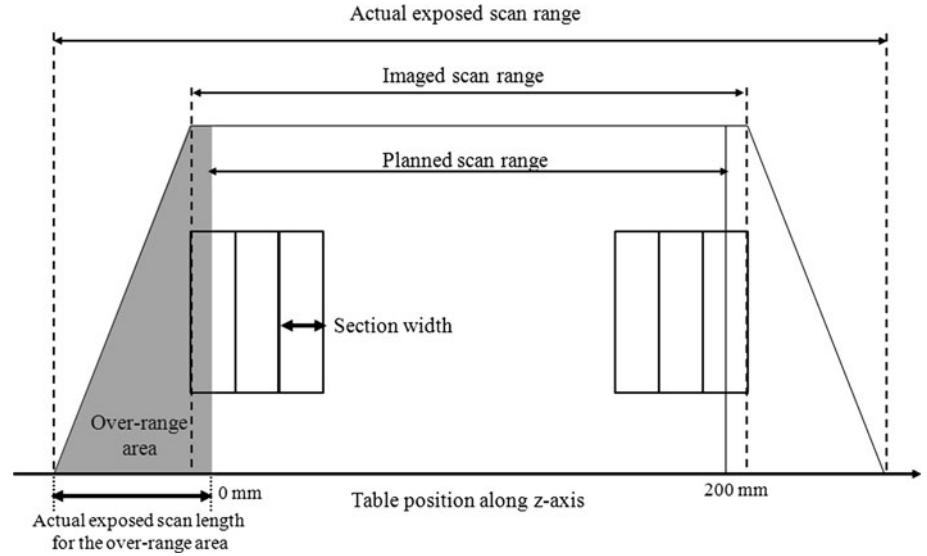
radiation dose profile curves along the z-axis, with and without the spiral dynamic z-collimator, were obtained with varying beam pitch and detector coverage.

We defined the "relative dose profile at iso-center" which was calculated from the mean value for each table position along the z-axis was divided by the mean value at a table position of 0 mm and beam pitch of 0.6.

Finally, the dose-saving ratio was calculated as the ratio of the unnecessary over-range dose, with and without the spiral dynamic z-collimator:

$$\text{Dose-saving ratio} = ((Dz\_off - Dz\_on)/Dz\_off) \times 100\ (\%)$$

where Dz_on is the unnecessary over-range dose with the spiral dynamic z-collimator, and Dz_off is the unnecessary over-range dose without the spiral dynamic z-collimator. The unnecessary over-range dose with or without the spiral dynamic z-collimator was computed from summation of the dose values with 31 GRDs in consideration of out of range along the z-axis from the unnecessary dose. Here, we determined the beginning point of the actual exposed scan length by the following methods. First, fraction (f) of the measurements for 2 adjacent GRDs (m_i, m_{i+1}) along the z-axis was calculated of each table position, and the equation was as follows: $f = (m_{i+1} - m_i)/m_i \times 100\ (\%)$. Next, the table position ($t.p_{\_\max}$) corresponding to the maximum fraction calculated from 30 fractions was determined in each beam pitch and with and without the spiral dynamic z-collimator. Finally, the beginning point of the actual exposed scan length was defined as the table position at the outside of 12 mm (distance for 2 GRDs) from $t.p_{\_\max}$ in consideration of the gradual slope for actual exposed scan length without the spiral dynamic z-collimator.

3 Results

Figure 2a shows the relative dose profiles without the spiral dynamic z-collimator at different beam pitches with use of the 80.0 mm detector coverage. The zero position of the transverse axis corresponds to the beginning of the planned scan range. The actual exposed scan lengths for the over-range area were 108, 120, and 126 mm, corresponding to beam pitches of 0.60, 0.80, and 0.99, respectively. The unnecessary dose for the over-range area increased with increasing beam pitch. With the spiral dynamic z-collimator, the actual exposed scan lengths for the over-range area were shorter than without it (see Fig. 1); and the values of the actual exposed scan length were 48, 66 and 84 mm, corresponding to beam pitches of 0.60, 0.80, and 0.99, respectively (Fig. 2b). In the over-range area for detector coverage of 80.0 mm, the dose-saving ratios for beam pitches of 0.60, 0.80, and 0.99 were 35.07, 24.76, and 13.51%, respectively (Table 1).

Figure 3a shows the relative dose profiles without the spiral dynamic z-collimator at different beam pitches with use of the 40.0 mm detector coverage. The actual exposed scan lengths for the over-range area were 54, 60, and 66 mm, corresponding to beam pitches of 0.60, 0.80, and 0.99 (Fig. 3a). In contrast, when we use the spiral dynamic z-collimator, the actual exposed scan length for the over-range area were shorter (30 mm, beam pitch 0.60; 36 mm, beam pitch 0.80; and 42 mm, beam pitch 0.99) than that without it (Fig. 3b). The unnecessary dose for the over-range area increased with increasing beam pitch, and this trend was the same as the detector coverage of 80.0 mm. In the over-range area, the dose-saving ratios with the detector coverage of 40.0 mm had the highest value of 27.23% with a low beam pitch of 0.60, and it decreased with increasing beam pitch (Table 1).
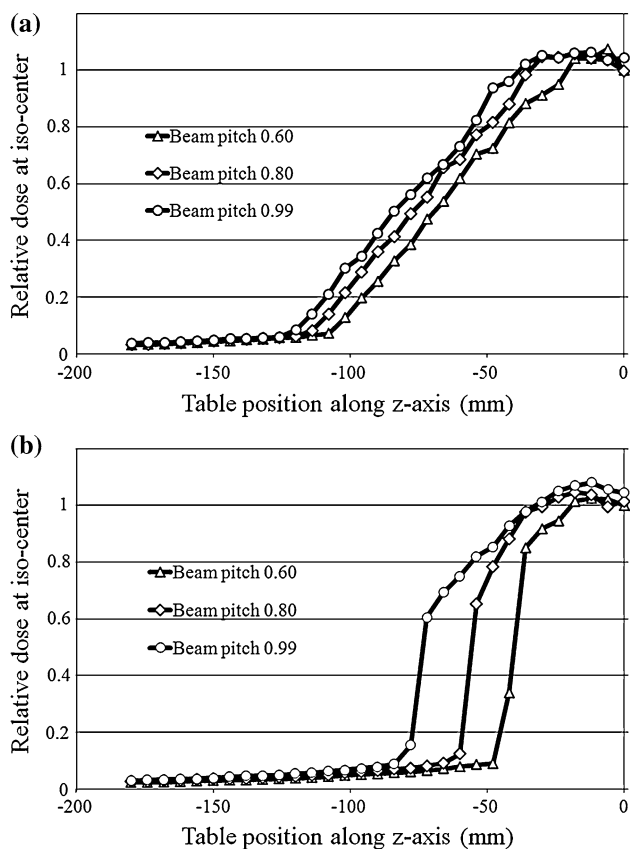
(a)

(b)

Fig. 2 a Relative dose profiles at over-range without a spiral dynamic z-collimator at different beam pitches with use of 80.0 mm detector coverage. b Relative dose profiles at over-range with a spiral dynamic z-collimator at different beam pitches with use of 80.0 mm detector coverage

(a)

(b)

Fig. 3 a Relative dose profiles at over-range without a spiral dynamic z-collimator at different beam pitches with use of 40.0 mm detector coverage. b Relative dose profiles at over-range with a spiral dynamic z-collimator at different beam pitches with use of 40.0 mm detector coverage

vs. 66 mm corresponding to beam pitches of 0.60, 0.80, and 0.99).

4 Discussion

The spiral dynamic z-collimator is useful for reducing the unnecessary dose for the over-range area. The unnecessary dose for the over-range area technically includes the two parts of "over-ranging" and "over-beaming". Over-ranging is the increase in the dose-length product (DLP) due to the additional rotations at the beginning and at the end of a spiral scan required for data interpolation to reconstruct the first and the last slices of the imaged body region. Over-ranging is reconstruction-algorithm specific, and its length generally increases with collimation and pitch [5] (Fig. 4). Over-beaming is the X-ray beam incident on the patient extends beyond the active detector area. From our results, when helical CT scanning with a detector coverage of 80.0 mm with the spiral dynamic z-collimator is needed, the unnecessary dose for the over-range area can be

Table 1 Dose-saving ratio (%) with and without the spiral dynamic z-collimator at a detector coverage of 80.0 and 40.0 mm

Detector coverage (mm)	Beam pitch		
	0.60	0.80	0.99
80.0	35.07	24.76	13.51
40.0	27.23	25.79	19.84

At the same beam pitch, the actual exposed scan length for the over-range area for detector coverage of 80.0 mm was longer than that for detector coverage of 40.0 mm, both with and without the spiral dynamic z-collimator, and the unnecessary dose at the detector coverage of 80.0 mm was also increased more than that for detector coverage of 40.0 mm. In a comparison of the detector coverage of 80.0 mm with the spiral dynamic z-collimator and 40.0 mm without it, the actual exposed scan length for the over-range area with the spiral dynamic z-collimator was almost the same as without it at the same beam pitch (80.0 mm coverage with the spiral dynamic z-collimator vs. 40.0 mm without it: 48 vs. 54 mm, 66 vs. 60 mm, 84
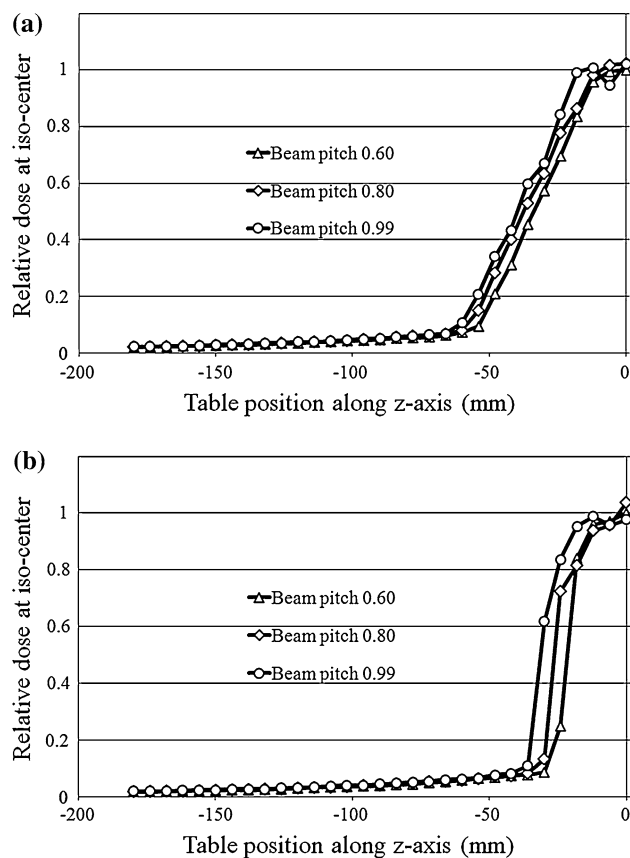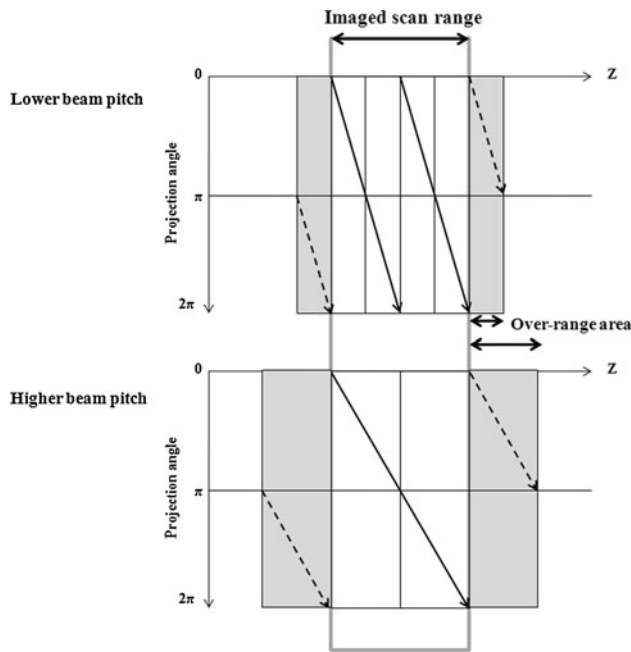
Fig. 4 Simple schematic of interpolation algorithm at different beam pitches. In general, an extra half rotation is required both at the beginning and at the end of the scan. Despite the same image scan range, the over-range area increases with increasing beam pitch and the unnecessary dose also increases
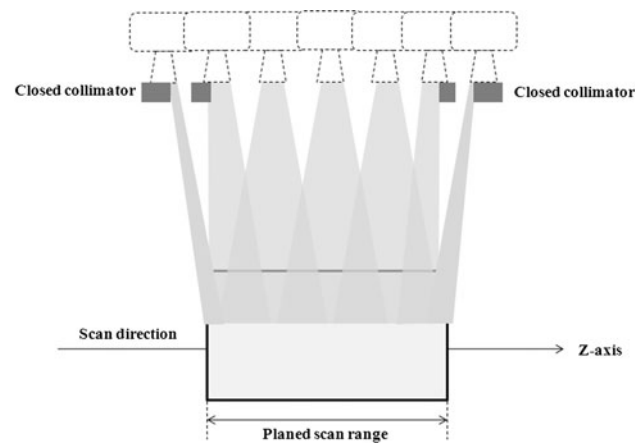

Fig. 5 Movement diagram of the spiral dynamic z-collimator. The collimator is closed until the beam is in front of the planned scan range. Then it opens only on the side entering the planned scan range until it is fully opened. At the end of the scan, the leading edge of the collimator closes when it leaves the planned scan range

controlled so as to achieve the same level of detector coverage of 40.0 mm without the spiral dynamic z-collimator. In other words, 128-detector row CT with a spiral dynamic z-collimator can scan rapidly and widely and can equalize the dose in the over-range area compared with conventional 64-detector row CT.

For fixed z-collimation, the collimator is fully open in the form of the sequential frames of a movie. As the beam moves toward the start of the prescribed planned scan volume, the accumulated dose produces the slanted side of a trapezoid. For the spiral dynamic z-collimator, however, the collimator is closed until the beam is in front of the planned scan range. Then it opens only on the side entering the planned scan range until it is fully opened. At the end of the scan, the leading edge of the collimator closes when it leaves the planned scan range. Thus, the dose profile curve becomes closer to being rectangular, resembling a sequential scan (Fig. 5). Christner et al. [9] reported, using another vendor's z-collimator, that the reduction in total incident radiation in the air at the iso-center varied between 27% (pitch 0.5) and 46% (pitch 1.5) for a scan length of 20 mm, respectively. They concluded that the percentage of the dose reductions was greatest for the shorter scan lengths and greater pitch values. This is different from our results (see Table 1). The reported dose-saving ratio is assumed to depend on the results from the combined *fixed* unnecessary over-range dose with a spiral dynamic

z-collimator (f_Dz_on) and unnecessary over-range dose without it (Dz_off); the equation is $1 - (f\_Dz\_on/Dz\_off)$. With increasing beam pitch, "Dz_off" increases and "f_Dz_on" remains constant. Consequently, the dose-saving ratio increases as the beam pitch increases. In contrast, our use of the spiral dynamic z-collimator changes the precision of the collimator corresponding to the beam pitch. In particular, a lower beam pitch enables fine control and reduces the unnecessary over-range dose more when compared with a higher beam pitch. Thus, our dose-saving ratio increases with decreasing beam pitch.

In scanning with abdominal CT, the spiral dynamic z-collimator is especially effective in reducing the radiation dose in the over-range area. This is because the abdominal CT scan usually requires plain (non-enhanced) and multiphase CT images with iodine contrast media [13, 14]. The radiation dose for the over-range area increases in addition to any increase of the radiation dose within the planned scan range. Consequently, a spiral dynamic z-collimator can lead to a reduction in the exposure of critical organs such as the female breast and human gonads [15, 16]. For instance, in studies of living related donors of liver transplantation, it is reported that they are essentially normal and relatively young people who are relatively radiosensitive compared with elderly people [17, 18]. In general, with use of the 128-detector row CT, the scan time for a planned scan is shorter than that of 64-detector row CT due to the wide detector coverage. If the timing of the peak enhancement of iodine contrast cannot be obtained due to a shorter scan time on 128-detector CT [19–21], we recommend the setting of a shorter beam pitch so as to make the equivalent total scan time the same as that of 64-detector CT. This allows a reduction in the radiation

dose from the over-range area and an improvement in the image quality because of the increase of the sampling view number [22].

This study has some limitations. First, we measured the excess dose for the over-range areas from the beginning of the actual exposed scan range to the beginning of the planned scan range with GRDs. Ideally, although the actual exposed scan dose from the beginning to the end of the actual exposed scan range may be needed, in practice it is difficult to measure the whole region because of the number of GRDs. However, we believe that reliable information is obtained about the unnecessary dose for the over-range area with and without the spiral dynamic z-collimator. Second, we did not use a beam pitch over 1.0 in consideration of the clinical situation. A study is now ongoing, and we need the assessment of a spiral dynamic z-collimator for high-beam pitch in the near future.

In conclusion, the spiral dynamic z-collimator is important for a reduction in the unnecessary over-range dose and makes it possible to reduce the unnecessary dose by means of a lower beam pitch.

References

1. Tzedakis A, Damilakis J, Perisinakis K, Stratakis J, Gourtsoyiannis N. The effect of z overscanning on patient effective dose from multidetector helical computed tomography examinations. Med Phys. 2005;32:1621–9.

2. Nicholson R, Fetherston S. Primary radiation outside the imaged volume of a multislice helical CT scan. Br J Radiol. 2002;75:518–22.

3. Theocharopoulos N, Damilakis J, Perisinakis K, Gourtsoyiannis N. Energy imparted-based estimates of the effect of z overscanning on adult and pediatric patient effective doses from multi-slice computed tomography. Med Phys. 2007;34:1139–52.

4. Tzedakis A, Damilakis J, Perisinakis K, Karantanas A, Karabekios S, Gourtsoyiannis N. Influence of z overscanning on normalized effective doses calculated for pediatric patients undergoing multidetector CT examinations. Med Phys. 2007;34:1163–75.

5. van der Molen AJ, Geleijns J. Overranging in multisection CT: quantification and relative contribution to dose—comparison of four 16-section CT scanners. Radiology. 2007;242:208–16.

6. Cohnen M, Poll LJ, Puettmann C, Ewen K, Saleh A, Modder U. Effective doses in standard protocols for multi-slice CT scanning. Eur Radiol. 2003;13:1148–53.

7. Flohr TG, Schaller S, Stierstorfer K, Bruder H, Ohnesorge BM, Schoepf UJ. Multi-detector row CT systems and image-reconstruction techniques. Radiology. 2005;235:756–73.

8. Taguchi K, Aradate H. Algorithm for image reconstruction in multi-slice helical CT. Med Phys. 1998;25:550–61.

9. Christner JA, Zavaletta VA, Eusemann CD, Walz-Flannigan AI, McCollough CH. Dose reduction in helical CT: dynamically adjustable z-axis X-ray beam collimation. AJR Am J Roentgenol. 2010;194:W49–55.

10. Walker MJ, Olszewski ME, Desai MY, Halliburton SS, Flamm SD. New radiation dose saving technologies for 256-slice cardiac computed tomography angiography. Int J Cardiovasc Imaging. 2009;25:189–99.

11. Mahesh M, Scatarige JC, Cooper J, Fishman EK. Dose and pitch relationship for a particular multislice CT scanner. AJR Am J Roentgenol. 2001;177:1273–5.

12. Rah J-E, Hong J-Y, Kim G-Y, Kim Y-L, Shin D-O, Suh T-S. A comparison of the dosimetric characteristics of a glass rod dosimeter and a thermoluminescent dosimeter for mailed dosimeter. Radiat Meas. 2009;44:18–22.

13. Baron RL. Understanding and optimizing use of contrast material for CT of the liver. AJR Am J Roentgenol. 1994;163:323–31.

14. Awai K, Takada K, Onishi H, Hori S. Aortic and hepatic enhancement and tumor-to-liver contrast: analysis of the effect of different concentrations of contrast material at multi-detector row helical CT. Radiology. 2002;224:757–63.

15. Hurwitz LM, Yoshizumi TT, Reiman RE, Paulson EK, Frush DP, Nguyen GT, Toncheva GI, Goodman PC. Radiation dose to the female breast from 16-MDCT body protocols. AJR Am J Roentgenol. 2006;186:1718–22.

16. Hohl C, Mahnken AH, Klotz E, Das M, Stargardt A, Muhlenbruch G, Schmidt T, Gunther RW, Wildberger JE. Radiation dose reduction to the male gonads during MDCT: the effectiveness of a lead shield. AJR Am J Roentgenol. 2005;184:128–30.

17. Lee SS, Kim TK, Byun JH, Ha HK, Kim PN, Kim AY, Lee SG, Lee MG. Hepatic arteries in potential donors for living related liver transplantation: evaluation with multi-detector row CT angiography. Radiology. 2003;227:391–9.

18. Schroeder T, Nadalin S, Stattaus J, Debatin JF, Malago M, Ruehm SG. Potential living liver donors: evaluation with an all-in-one protocol with multi-detector row CT. Radiology. 2002;224:586–91.

19. Frederick MG, McElaney BL, Singer A, Park KS, Paulson EK, McGee SG, Nelson RC. Timing of parenchymal enhancement on dual-phase dynamic helical CT of the liver: how long does the hepatic arterial phase predominate? AJR Am J Roentgenol. 1996;166:1305–10.

20. Awai K, Hiraishi K, Hori S. Effect of contrast material injection duration and rate on aortic peak time and peak enhancement at dynamic CT involving injection protocol with dose tailored to patient weight. Radiology. 2004;230:142–50.

21. Goshima S, Kanematsu M, Kondo H, Yokoyama R, Miyoshi T, Nishibori H, Kato H, Hoshi H, Onozuka M, Moriyama N. MDCT of the liver and hypervascular hepatocellular carcinomas: optimizing scan delays for bolus-tracking techniques of hepatic arterial and portal venous phases. AJR Am J Roentgenol. 2006;187:W25–32.

22. Barrett JF, Keat N. Artifacts in CT: recognition and avoidance. Radiographics. 2004;24:1679–91.